Effects of Forced Expression of an NH_2-terminal Truncated β-Catenin on Mouse Intestinal Epithelial Homeostasis

Melissa H. Wong,* Bonnee Rubinfeld,‡ and Jeffrey I. Gordon*

*Department of Molecular Biology and Pharmacology, Washington University School of Medicine, St. Louis, Missouri 63110; and ‡Onyx Pharmaceuticals, Richmond, California 94806

Abstract. β-Catenin functions as a downstream component of the Wnt/Wingless signal transduction pathway and as an effector of cell–cell adhesion through its association with cadherins. To explore the in vivo effects of β-catenin on proliferation, cell fate specification, adhesion, and migration in a mammalian epithelium, a human NH_2-terminal truncation mutant (ΔN89β-catenin) was expressed in the 129/Sv embryonic stem cell–derived component of the small intestine of adult C57Bl/6–ROSA26↔129/Sv chimeric mice. ΔN89β-Catenin was chosen because mutants of this type are more stable than the wild-type protein, and phenocopy activation of the Wnt/Wingless signaling pathway in *Xenopus* and *Drosophila.* ΔN89β-Catenin had several effects. Cell division was stimulated fourfold in undifferentiated cells located in the proliferative compartment of the intestine (crypts of Lieberkühn). The proliferative response was not associated with any discernible changes in cell fate specification but was accompanied by a three- to fourfold increase in crypt apoptosis. There was a marked augmentation of E-cadherin at the adherens junctions and basolateral surfaces of 129/Sv (ΔN89β-catenin) intestinal epithelial cells and an accompanying slowing of cellular migration along crypt-villus units. 1–2% of 129/Sv (ΔN89β-catenin) villi exhibited an abnormal branched architecture. Forced expression of ΔN89β-catenin expression did not perturb the level or intracellular distribution of the tumor suppressor adenomatous polyposis coli (APC). The ability of ΔN89β-catenin to interact with normal cellular pools of APC and/or augmented pools of E-cadherin may have helped prevent the 129/Sv gut epithelium from undergoing neoplastic transformation during the 10-mo period that animals were studied. Together, these in vivo studies emphasize the importance of β-catenin in regulating normal adhesive and signaling functions within this epithelium.

β-Catenin plays important roles in cell adhesion and cell signaling (for review see Miller and Moon, 1996; Nusse, 1997). The protein influences adhesion by providing a functional bridge between cadherins and the actin cytoskeleton. Calcium-dependent homotypic interactions between the extracellular domains of cadherins result in the formation of adhesion "zippers" between adjacent cells (Overduin et al., 1995; Shapiro et al., 1995). Although these interactions help define the specificity of cellular interactions, they are not sufficient for productive adhesion. Productive adhesion at the adherens junction is accomplished by the binding of β-catenin to the conserved cytoplasmic domains of cadherins and to the cytoplasmic protein α-catenin. α-Catenin, in turn, is linked to the cytoskeleton via its interactions with other proteins (e.g., actinin; Nagafuchi and Takeichi, 1988; Ozawa et al., 1989, 1990; Aberle et al., 1994; Hinck et al., 1994; Jou et al., 1995; Rimm et al., 1995).

β-Catenin is also a critical downstream component of the Wnt signal transduction pathway in vertebrates. In the absence of a Wnt signal, serine/threonine phosphorylation by glycogen synthase kinase-3 (GSK-3)[1] leads to rapid degradation of cytoplasmic pools of β-catenin through a ubiquitin–proteosome pathway (Miller and Moon, 1996;

Address all correspondence to Jeffrey I. Gordon, Department of Molecular Biology and Pharmacology, Box 8103, Washington University School of Medicine, 660 South Euclid Ave., St. Louis, MO 63110. Tel.: (314) 362-7243. Fax: (314) 362-7047. E-mail: jgordon@pharmdec.wustl.edu

1. *Abbreviations used in this paper*: β-gal, β-galactosidase; ΔN89β-catenin, NH_2-terminal truncation mutant of human β-catenin lacking amino acid residues 1–89; APC, adenomatous polyposis coli protein or gene; BrdU, 5′-bromo-2′deoxyuridine; Cy3, indocarbocyanine; DBA, *Dolichos biflorus* agglutinin; ES cell, embryonic stem cell; *Fabpl*, fatty acid binding protein gene; GSK-3, glycogen synthase kinase-3; hGH, human growth hormone gene; LEF-1, lymphocyte enhancing factor-1; PLP, periodate-lysine-paraformaldehyde; RT, reverse transcriptase; TAg, T antigen; Tcf, T-cell factor; X-Gal, 5-bromo-4-chloro-3-indolyl β-D-galactoside.

Munemitsu et al., 1996; Yost et al., 1996; Aberle et al., 1997; Cadigan and Nusse, 1997). In contrast, stimulation of the Wnt pathway leads to repression of GSK-3 (Noordermeer et al., 1994; Cook et al., 1996), decreased β-catenin phosphorylation, and enhanced protein stability. The resulting augmentation of β-catenin pools facilitates formation of complexes between β-catenin and high mobility group box transcription factors (T-cell factor [Tcf] and lymphocyte enhancing factor-1 [LEF-1]); Behrens et al., 1996; Huber et al., 1996). In the nucleus, β-catenin functions to coactivate transcription of largely unspecified gene targets (Behrens et al., 1996; Huber et al., 1996; Molenaar et al., 1996; Brunner et al., 1997; Riese et al., 1997; van de Wetering et al., 1997).

Studies in genetically manipulatable nonvertebrate species as well as nonmammalian vertebrate organisms have shown that β-catenin–mediated signaling affects axis formation and cell fate specification (McCrea et al., 1993; Heasman et al., 1994; Funayama et al., 1995; Cox et al., 1996; Molenaar et al., 1996). However, attempts to test the in vivo functions of β-catenin in mammals have been hampered by the fact that mice homozygous for a genetically engineered null allele die during early embryogenesis (Haegel et al., 1995).

One function of β-catenin in mammalian cell lineages that has been recently explored is its role in oncogenic transformation. Several reports have emphasized that the tumor suppressor adenomatous polyposis coli (APC) functions to affect intestinal tumorigenesis through its regulation of β-catenin signaling. Mutations in APC lead to intestinal adenomas and adenocarcinoma in mice and humans (Su et al., 1992; for review see Kinzler and Vogelstein, 1996; Shibata et al., 1997). The interaction between β-catenin and APC is enhanced when APC is phosphorylated by GSK-3, thereby promoting β-catenin turnover (Su et al., 1993; Rubinfeld et al., 1993, 1996). When APC is absent, or is mutated so that β-catenin binding is impaired, cytosolic pools of β-catenin are elevated, and β-catenin–Tcf signaling is induced (Munemitsu et al., 1995; Korinek et al., 1997; Morin et al., 1997). Additional evidence for the importance of β-catenin signaling in tumorigenesis comes from the observation that some human colorectal neoplasms with wild-type *APC* genes have mutations in β-catenin (Ilyas et al., 1997; Morin et al., 1997). Some of these mutations affect potential sites for GSK-3 phosphorylation and therefore are likely to lead to augmented pools of β-catenin.

In addition to its role in gut neoplasia, there are other reasons why the self-renewing adult intestinal epithelium represents an attractive mammalian model for studying the in vivo functions of β-catenin. Fundamental developmental processes such as cellular proliferation, lineage allocation, differentiation, migration/adhesion, and death are continuously expressed in well-defined domains of the small intestine's anatomically distinct crypt-villus units. Proliferation is confined to flask-shaped mucosal invaginations known as crypts of Lieberkühn. In the adult mouse, each of the small intestinal crypts contains one or more active multipotent stem cells functionally anchored near its base (Loeffler et al., 1993; Potten et al., 1997). These stem cells give rise to daughters that undergo four to six rounds of cell division in the midportion of the crypt and are allocated to four principal epithelial cell lineages. Each lineage completes its differentiation during a highly organized, rapid migration. Absorptive enterocytes (accounting for >80% of the epithelial population), mucus-producing goblet cells, and enteroendocrine cells exit the crypt and move up an adjacent finger-like structure (the villus) in vertical coherent columns (Schmidt et al., 1985; Hermiston et al., 1996). Cells are removed from the villus tip by apoptosis and/or extrusion into the lumen (Hall et al., 1994). The entire sequence is completed in 3–5 d (Cheng and Leblond, 1974*a–c*; Cheng, 1974*a*). Members of the Paneth cell lineage differentiate as they move downward to the base of the crypt where they are removed after an ~20-d residence (Cheng, 1974*b*). E-Cadherin, the principal intestinal epithelial cadherin, β-catenin, α-catenin, and APC are expressed in cells distributed along the length of crypt-villus units (Hermiston et al., 1996; Näthke et al., 1996; Wong et al., 1996). The importance of cadherins and their related proteins to normal intestinal epithelial homeostasis was established when a dominant-negative cadherin was expressed in the 129/Sv component of C57Bl/6↔129/Sv chimeric mouse gut. Cell–cell and cell–substratum interactions were disrupted leading to alterations in migration rates, diminished cell survival, breakdown of mucosal barrier function, inflammatory bowel disease, and adenoma formation (Hermiston et al., 1995*a*,*b*).

In the present report, we have examined the effects of forced expression of a human β-catenin lacking its NH_2-terminal 89 residues (ΔN89β-catenin) on the small intestinal epithelium of C57Bl/6↔129/Sv chimeric mice. ΔN89β-Catenin was chosen for several reasons. Studies in cultured cell lines indicated that this mutant, which lacks putative GSK-3 phosphorylation sites (Yost et al., 1996), has a longer half-life than the wild-type protein, leading to its accumulation both as a stable monomer and as a complex with APC (Munemitsu et al., 1996; Barth et al., 1997; Rubinfeld et al., 1997). The NH_2-terminal truncation does not appear to affect binding to E-cadherin, does not involve the domains involved in binding α-catenin or Tcf (Munemitsu et al., 1996; Orsulic and Peifer, 1996), and preserves all of the protein's structurally and functionally important *armadillo* repeats (Huber et al., 1997). Finally, studies in *Drosophila* and *Xenopus* had shown that NH_2-terminal truncation mutants of β-catenin promote signaling (Yost et al., 1996; Pai et al., 1997), whereas expression in cultured mammalian epithelial cells affects cell migration (Pollack et al., 1997). Thus, we anticipated that ΔN89β-catenin would allow us to examine the effects of β-catenin on both signaling and adhesion/migration in the mouse intestine.

Materials and Methods

Generation of Chimeric-Transgenic Mice

pL596hGHpNeoΔB_2 (Hermiston et al., 1996) contains nucleotides -596 to +21 of the rat fatty acid binding protein gene (*Fabpl*) upstream of nucleotides +3 to +2150 of the human growth hormone gene (hGH). A phosphoglycerate kinase (*pgk)* neomycin resistance selection cassette is located just downstream of *Fabpl*-hGH. pL596hGHpNeoΔB_2 was cleaved at its unique BamHI site located at nucleotide +3 of hGH, and a double-stranded oligonucleotide containing flanking BamHI sites and internal KpnI and XbaI sites (5′-GATCCGGTACCATCGATGGGTCTAGAG-3′) was inserted. The resulting DNA, pLFhGHpNeoK contains a unique KpnI site for subcloning cDNAs into exon 1 of hGH. pCANβ-cateninΔN_{90}c.62

(provided by P. Polakis, Onyx Pharmaceuticals, Richmond, CA) contains a DNA insert encoding myc-tagged human ΔN89β-catenin. A 2.2-kb KpnI/XbaI fragment from pCANβ-cateninΔN_{90}c.62 was subcloned into KpnI/XbaI–digested pLFhGHpNeoK DNA, creating pLFΔN89βcat. The 6.9-kb *Fabpl*–ΔN89βcat-hGH–*pgk*neo insert in pLFΔN89βcat was excised with SacII, purified by gel electrophoresis, and then electroporated into D3 129/Sv ES cells (Hermiston et al., 1995*a*). Stably transfected embryonic stem (ES) cell clones were injected into C57Bl/6 ROSA26$^{+/-}$ blastocysts (Wong et al., 1996) to produce B6-ROSA26↔129/Sv(ΔN89β-catenin) chimeric-transgenic mice. Chimeras generated from three of the cell lines were analyzed at 6 wk, 6 mo, and 10 mo of life. Their 129/Sv contribution ranged from 20 to 80% based on coat color. The presence of ROSA26 in chimeras was established using a PCR protocol (The Jackson Laboratory, Bar Harbor, ME) and tail genomic DNA. Independent confirmation was obtained by staining segments of tail with 5-bromo-4-chloro-3-inodyl β-D-galactoside (X-Gal) (Wong et al., 1996). Nontransfected D3 ES cells were used to generate B6-ROSA26↔129/Sv chimeras (referred to as "normal control" chimeras in this study).

All animals were maintained in microisolator cages under a strict 12-h light cycle and fed a standard chow diet ad libitum (Pico Lab Rodent Diet 20; Purina Mills, Inc., St. Louis, MO). Routine screening of sentinel animals indicated that all chimeric mice were free of pathogens.

Assays for Transgene Expression

Reverse Transcriptase-PCR. Total cellular RNA was isolated from the proximal, middle, and distal thirds of the small intestine and the skeletal muscle of 6-wk-old B6-ROSA26↔129/Sv(ΔN89β-catenin) mice using the RNeasy kit (QIAGEN Inc., Santa Clarita, CA). Oligo dT-primed cDNA was generated from DNA-free intestinal RNA. Four separate PCR reactions contained one of four primers that recognize human β-catenin sequences (5′-TTGATGGGCTGCCAGTACTG-3′, 5′-CTACCAGTTGTGGTTAAGC-3′, 5′-TGCACATCAGGATACCCAGC-3′, or 5′-TATTGAAGCTGAGGGAGCCACAGC-3′), and a primer that recognizes sequences derived from exon 2 of the hGH gene (5′-GGCAGAGCAGGCCAAAAGCC-3′). The following conditions were used for PCR: denaturation at 95°C for 1 min; annealing at 65°C for 1 min; and extension at 72°C for 2 min using standard buffer and salt conditions (total = 30 cycles). Control reactions contained intestinal RNA prepared from normal control B6-ROSA26↔129/Sv chimeras.

Immunoblots. A segment was taken from the middle of the small intestine of B6-ROSA26↔129/Sv(ΔN89β-catenin) and B6-ROSA26↔129/Sv mice and frozen immediately. After lyophilization, total cellular proteins were extracted by homogenizing the sample at 60°C in 1 ml of denaturation buffer (Laemmli, 1970) supplemented with protease inhibitors (1 μg/ml leupeptin, 1 μg/ml pepstatin, 4 mM 4-[2-aminoethyl]-benzensulfonyl fluoride hydrochloride, 1 μg/ml aprotinin, 1 mM EDTA). Insoluble debris was removed by centrifugation at 12,000 *g* for 10 min. The protein concentration in the resulting supernatant was defined (Hill and Straka, 1988). Samples of protein (100 μg) were fractionated by SDS-PAGE and electrophoretically transferred to polyvinylidene difluoride membranes. The membranes were stained with Ponceau S to verify successful transfer, preincubated for 1 h at 24°C with blocking buffer (PBS supplemented with 1% wt/vol gelatin and 0.5% vol/vol Tween-20) (Sigma Chemical Co., St. Louis, MO), and then probed for 1 h at 24°C with one of the following antibody preparations: (*a*) affinity-purified rabbit anti–c-myc epitope (MEQKLISEEDLN, 1:50 in PBS blocking buffer; Upstate Biotechnology Inc., Lake Placid, NY); (*b*) rabbit antisera raised against the COOH-terminal 14 residues of human/mouse β-catenin (PGDSNQLAWFDTDL, 1:200; provided by J. Nelson, Stanford University, Stanford, CA); and (*c*) rabbit anti-actin (1:5,000; Sigma Chemical Co.). Antigen–antibody complexes were detected using the reagents and protocols included in the Western Light kit® from Tropix, Inc. (Bedford, MA).

Preparation and Staining of Intestinal Wholemounts

The small intestine was removed en bloc from mice immediately after killing and divided in half. Each half was gently flushed with ice-cold PBS, followed by periodate-lysine-paraformaldehyde (PLP; McLean and Nakane, 1974). Each half was opened with a single longitudinal incision along its mesenteric side and then subdivided into three equal parts. Each part was pinned onto a wax substrate and then fixed in PLP for 1 h at 24°C. The samples were washed with PBS (three cycles of 5 min each), incubated in 20 mM DTT/20% ethanol per 150 mM Tris-HCl, pH 8.0, for 45 min to remove mucus, and then washed again with PBS (three cycles). The epithelium was then genotyped by incubating all parts of the small intestine for 12 h at 4°C in PBS containing 2 mM X-Gal, 4 mM potassium ferricyanide, 4 mM potassium ferrocyanide, and 2 mM $MgCl_2$, final pH 7.6. The six regions of the small intestine were analyzed and photographed using a stereoscope (model SHZ10; Olympus, Tokyo, Japan), and then placed in 2% agar/PBS. Care was taken to preserve the orientation of crypt-villus units in each region while it was embedded in paraffin. Serial sections (5–8-μm-thick) were prepared along the cephalocaudal axis of each region (n = 300–500/region per animal).

Quantitation of Apoptotic and M-Phase Cells

Sections, prepared from the two middle regions of X-Gal–stained small intestine (jejunum), were counterstained with hematoxylin and eosin. M-phase and apoptotic cells were identified in each of these regions by their characteristic morphology (Hall et al., 1994; Coopersmith et al., 1997). Two 6-mo-old animals from each of three B6-ROSA26↔129/Sv(ΔN89β-catenin) lines and three 6-mo-old B6-ROSA26↔129/Sv mice were studied. A minimum of 200 well-oriented B6-ROSA26 and 200 well-oriented 129/Sv crypts were counted per mouse (well-oriented = crypt-sectioned parallel to the crypt-villus axis with Paneth cells represented at the crypt base and an unbroken epithelial column extending from the crypt base to the villus tip). A crypt had to be located within juxtaposed patches of B6-ROSA26 and 129/Sv crypt-villus units to be tallied. Each animal served as its own control; data from individual mice were expressed as the average number of M-phase (or apoptotic) cells per 129/Sv crypt divided by the average number of M-phase or apoptotic cells per B6-ROSA26 crypt. All slides were analyzed in a single-blinded fashion. Values obtained from animals from each line were averaged. Statistical analyses were conducted using unpaired Student's *t*-test.

Quantitation of Branched Villi

Sections obtained from the middle portions of the small intestine (see above), were stained with nuclear fast red and scored for the presence of branched villi. A minimum of 500–1000 villi in juxtaposed patches of B6-ROSA26 and 129/Sv crypt-villus units were scored per animal (n = two 6-mo-old mice/line of B6-ROSA26↔129/Sv[ΔN89β-catenin] chimeric-transgenic animals; n = three age-matched B6-ROSA26↔129/Sv normal control chimeras). Branched villi were identified using the following criteria: (*a*) a villus had to have a continuous layer of epithelium over all of its branches; (*b*) immunostaining of an adjacent serial section with rabbit anti-laminin sera had to reveal a continuous ribbon of basement membrane underlying the uninterrupted epithelial sheet; and (*c*) the branched villus had to be present in adjacent serial sections.

Single and Multilabel Immunohistochemistry

Mice were injected with 5′-bromo-2′deoxyuridine (BrdU, 120 mg/kg body weight; Sigma Chemical Co.) and 5′-fluoro-2′-deoxyuridine (12 mg/kg; Sigma Chemical Co.) 60 h before killing. The entire small intestine was removed en bloc and wholemounts were prepared, fixed in PLP, stained with X-Gal, embedded in paraffin as described above, and then cut into 5-μm-thick sections. Alternatively, the middle third of the small intestine was flushed with PBS, fixed in PLP for 1 h at 24°C, and then flushed and embedded with O.C.T.(Miles Inc., Kankakee, IL). The embedded tissue was then frozen in Cytocool (VWR, St. Louis, MO) and 6–8-μm-thick sections were prepared.

Protocols used for single- and multilabel immunohistochemical studies have been described in our earlier publications (Hermiston et al., 1995*a*; 1996). PLP-fixed frozen sections of jejunum were stained with a 19-member panel of antibodies: (*a*) affinity-purified rabbit anti–*Escherichia coli* β-galactosidase (β-gal) (1:500; 5′→3′ Inc., Boulder, CO); (*b*) rabbit anti–β-catenin sera (see above, final dilution in PBS/blocking buffer = 1:500); (*c*) affinity-purified rabbit anti–c-myc (see above, 1:100); (*d*) affinity-purified rabbit antibodies raised against amino acids 1034–2130 of human APC (APC2, a gift of P. Polakis; Näthke et al., 1996; Wong et al., 1996); (*e*) affinity-purified rabbit anti–α-catenin (1:500; gift of J. Nelson); (*f*) a monoclonal rat antibody to E-cadherin (1:1,000; Sigma Chemical Co.; Hermiston et al., 1995*a*); (*g*) rat anti–ZO-1 (polyclonal antibodies, 1:50; Chemicon International, Inc., Temecula, CA); (*h*) rabbit anti-laminin (1:1,000; Chemicon International Inc.); (*i*) rabbit anti-mouse fibronectin (1:1,000; Chemicon International Inc.); (*j*) rabbit anti-mouse collagen type IV (1:1,000; Chemicon International Inc.); (*k*) rat anti-mouse β_1 integrin (1:500; PharMingen, San Diego, CA); (*l*) rat anti-mouse β_7 integrin (1:500;

PharMingen); (*m*) rat anti-mouse β_4 integrin (1:500; PharMingen); (*n*) rat anti-mouse α_6 integrin (1:500; PharMingen); (*o*) goat anti-BrdU (1:1,000; Cohn et al., 1992); (*p*) rabbit anti-serotonin (1:1,000, a marker of the predominant enteroendocrine subpopulation in the adult mouse intestine; Incstar, Stillwater, MN); (*q*) rabbit anti-chromagranin A (1:1,000, a general marker of enteroendocrine cells; Incstar); and (*r*) rabbit anti-liver fatty acid binding protein (1:1,000, an enterocyte lineage marker; Sweetser et al., 1988).

Antigen–antibody complexes were detected with indocarbocyanine (Cy3)- or FITC-conjugated donkey anti–rabbit, anti–rat, or anti–goat Ig (1:500; Jackson ImmunoResearch Laboratories, Inc., West Grove, PA).

Analysis of the components of the diffuse gut–associated lymphoid tissue was performed on PLP-fixed frozen sections of jejunum. Antigen–antibody complexes were visualized using tyramide signal amplification as described previously (Garabedian et al., 1997).

PLP-fixed and X-Gal–stained sections of paraffin-embedded wholemounts were also incubated with a series of lectins (all used at a final concentration of 5 μg/ml PBS blocking buffer and detected according to Falk et al., 1994): (*a*) *Ulex europaeus* agglutinin 1 (carbohydrate specificity = Fucα1, 2Gal epitopes; lineage specificity = Paneth, goblet, and enteroendocrine cells; Sigma Chemical Co.); (*b*) Peanut (*Arachis hypogaea*) agglutinin (Galβ3GalNAc epitopes; all four epithelial lineages; Sigma Chemical Co.); (*c*) *Dolichos biflorus* agglutinin (GalNAcα3GalNAc and GalNAcα3Gal epitopes; Paneth and goblet cells plus enterocytes; Sigma Chemical Co.); (*d*) *Helix pomentia* agglutinin (α-GalNAc; GalNAcβ4Gal epitopes; Paneth and goblet cells; Sigma Chemical Co.); (*e*) Jacalin-1 (*Artrocarpus integrifolia* agglutinin; Galα6Gal; Galβ3GalNAc epitopes; enterocytes and goblet cells; E.Y. Laboratories, Inc., San Mateo, CA).

Stained sections were viewed with an Axiophot microscope (Carl Zeiss, Inc., Thornwood, NY) and/or model 2001 confocal microscope (Molecular Dynamics, Inc., Sunnyvale, CA). Scans in the confocal microscope were performed at 1-μm intervals.

Results

Generation of B6-ROSA26↔129/Sv(ΔN89β-Catenin) Chimeric Mice

129/Sv ES cells were stably transfected with a recombinant DNA consisting of nucleotides -596 to +21 of *Fabpl* (Sweetser et al., 1988) positioned upstream of an open reading frame encoding ΔN89β-catenin with an NH_2-terminal myc tag. The *Fabpl* transcriptional regulatory elements were selected because previous studies in neonatal and adult transgenic mice had shown that they could be used to direct expression of a variety of proteins to the region of small intestinal crypt containing the multipotent stem cell, and to all four of the stem cell's descendant cell lineages throughout the course of their differentiation (Trahair et al., 1989; Kim et al., 1993; Simon et al., 1993; Hermiston et al., 1996). Moreover, *Fabpl*-reporter transgene expression commences coincidently with initial cytodifferentiation of the intestinal epithelium in late fetal life and is sustained throughout adulthood, with highest levels of expression occurring in the middle third of the small bowel (jejunum).

Individual clones of stably transfected, *Fabpl*–NΔ89β-catenin ES cells, or control nontransfected ES cells, were injected into C57Bl/6-ROSA26 (B6-ROSA26) blastocysts (Friedrich and Soriano, 1991; Wong et al., 1996). There are several reasons why the resulting chimeras are well-suited for studying the effects of transgene expression on the gut. First, intestinal epithelial cells of each genotype are separated into anatomically distinct units. By the time gut morphogenesis is completed, all crypts in B6-ROSA26↔129/Sv chimeras are monoclonal; they contain either B6-ROSA26 or 129/Sv epithelial cells, but not a mixture of both (Wong et al., 1996). Several crypts surround the villus base and supply epithelial cells to each villus. Thus, the chimeric small intestine will contain patches of transgenic 129/Sv crypt-villus units and adjacent patches of normal (nontransgenic) B6-ROSA26 crypt-villus units. A villus located at the border of a patch of B6-ROSA26 crypts and a patch of 129/Sv crypts will be polyclonal, containing a vertical coherent column of transgenic epithelial cells emanating from a monoclonal 129/Sv crypt and an adjacent column of normal epithelial cells emanating from a monoclonal B6 crypt (Fig. 1, *A* and *B*). Second, genotyping is simple. All undifferentiated and differentiated epithelial cells in B6-ROSA26 patches produce *E. coli* β-gal (Wong et al., 1996). Therefore, the B6-ROSA26 component can be identified by staining the opened chimeric small intestine with X-Gal (see blue-stained villi in Fig. 1 *A*). The 129/Sv epithelium does not produce β-gal and can be identified, even in chi-

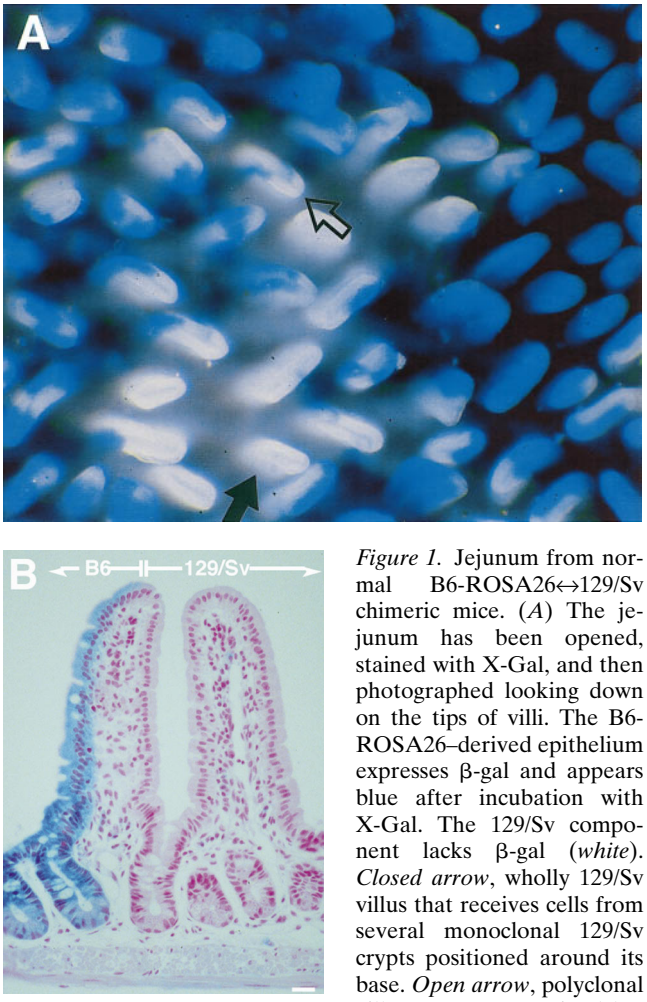

Figure 1. Jejunum from normal B6-ROSA26↔129/Sv chimeric mice. (*A*) The jejunum has been opened, stained with X-Gal, and then photographed looking down on the tips of villi. The B6-ROSA26–derived epithelium expresses β-gal and appears blue after incubation with X-Gal. The 129/Sv component lacks β-gal (*white*). *Closed arrow*, wholly 129/Sv villus that receives cells from several monoclonal 129/Sv crypts positioned around its base. *Open arrow*, polyclonal villus. It appears striped because it receives columns of β-gal–negative (*white*) cells from monoclonal 129/Sv crypts and β-gal–positive cells from monoclonal B6-ROSA26 crypts. (*B*) Paraffin-embedded section prepared from the same wholemount and stained subsequently with nuclear fast red. The villus on the left is polyclonal: it is supplied by a monoclonal B6-ROSA26 crypt that contains an entirely β-gal–positive population of blue cells and by a monoclonal 129/Sv crypt that only contains β-gal–negative cells. The villus on the right is only supplied by 129/Sv crypts. Bar, 25 μm.

meras with a low percentage 129/Sv contribution, by its white appearance. Third, regions of nontransgenic B6 epithelium serve as a critical internal control for defining the effects of the transgene's product. Since the small intestine is characterized by complex cephalocaudal variations in cell production and differentiation, it is critical that the control epithelial population be represented in a similar location as the genetically manipulated population. In the case of a polyclonal villus, the effect of the transgene can be defined by comparing 129/Sv and B6 cells located at a given cell stratum of a single villus positioned at a unique location along duodenal-ileal axis of an individual animal (Fig. 1 *B*).

Four independent *Fabpl*–ΔN89β-catenin ES cell lines were injected into B6-ROSA26 blastocysts to generate B6-ROSA26↔129/Sv(ΔN89β-catenin) chimeric-transgenic mice. Total RNA was isolated from the jejunum of 6-wk-old animals with 20–80% 129/Sv contribution (defined by coat color). Reverse transcriptase (RT)-PCR analysis revealed the expected sized product from the *Fabpl*–ΔN89β-catenin transgene in all four chimeric-transgenic lines (Fig. 2 *A*). The RT-PCR product was not present in RNA prepared from the jejunum of normal control B6ROSA26↔129/Sv chimeras produced from nontransfected ES cells, or in RNA isolated from the skeletal muscle of chimeric-transgenic animals (Fig. 2 *A*).

Transgene expression was independently confirmed by immunoblot analysis of total jejunal proteins isolated from 6-wk-old chimeric-transgenic and normal control chimeric mice with equivalent 129/Sv contributions. When the immunoblots were probed with antibodies that recognize the myc tag, an 80-kD protein corresponding to the predicted mass of myc–ΔN89β-catenin was detected in the jejunums of chimeric-transgenic but not control chimeric animals (Fig. 2 *B*). Duplicate blots were probed with polyclonal antibodies raised against a peptide derived from an absolutely conserved region of human and mouse β-catenin. The steady-state level of immunoreactive β-catenin species was severalfold higher in the jejunums of chimeric-transgenic mice compared with control chimeras (Fig. 2 *B*), consistent with successful forced expression of ΔN89β-catenin.

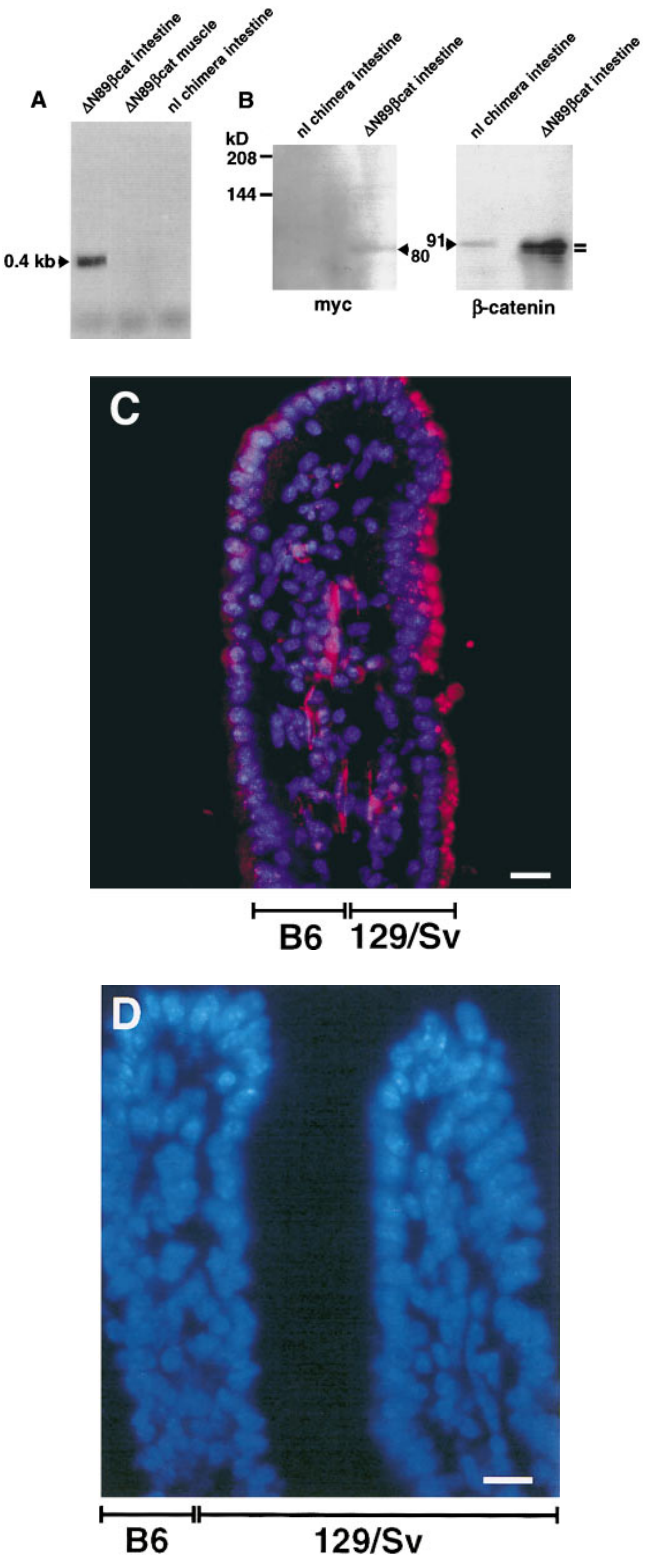

Figure 2. Evidence for expression of the *Fabpl*–ΔN89β-catenin transgene. (*A*) RT-PCR analysis of RNAs isolated from the jejunum and skeletal muscle of a 6-wk-old-chimeric-transgenic mouse (*ΔN89β-catenin*) and from the jejunum of a 6-wk-old chimera generated using nontransfected ES cells (*nl chimera*). The arrow points to the expected size of the product generated from ΔN89β-catenin mRNA. (*B*) Duplicate immunoblots are shown each containing total cellular proteins isolated from the jejunum of a 6-wk-old normal control B6-ROSA26↔129/Sv chimeric mouse and a 6-wk-old B6-ROSA26↔129/Sv(ΔN89β-catenin) chimeric-transgenic animal (both with 30–40% 129/Sv contribution based on coat color). The blot on the left of the panel was probed with antibodies that recognize the myc epitope tag present at the NH_2 terminus of the 80-kD ΔN89β-catenin mutant (*arrow*). The blot on the right of the panel was probed with antibodies raised against the COOH terminus of β-catenin (molecular mass of wild-type β-catenin = 91 kD). (*C*) PLP-fixed frozen section of a polyclonal villus from a B6-ROSA26↔129/Sv(ΔN89β-catenin) mouse. The section was incubated with affinity-purified rabbit antibodies to the myc tag, Cy3-tagged donkey anti–rabbit Ig, and the nuclear stain bis-benzimide (*dark blue*). Myc-tagged ΔN89β-catenin (*magenta*) is prominently represented in 129/Sv but not B6-ROSA26 villus epithelial cells. (Genotyping was accomplished by staining an adjacent serial section with antibodies to β-gal.) (*D*) Section of a polyclonal villus from a normal chimeric mouse stained with the same reagents as in *C*. 129/Sv epithelial cells lack the transgene, and therefore do not contain any myc-tagged protein. Bars: (*C* and *D*) 25 μm.

A final confirmation of transgene expression was provided by immunohistochemistry. Serial sections of chimeric-transgenic and normal chimeric jejunums were stained with antibodies raised against the myc tag and β-gal. In chimeric-transgenic mice, immunoreactive myc was present in β-gal–negative 129/Sv epithelial cells, but not in β-gal–positive B6-ROSA26 epithelial cells (Fig. 2 *C*). In normal control chimeras, the myc tag was not detectable in either 129/Sv or B6-ROSA26 epithelium (Fig. 2 *D*).

Villus Branching in 129/Sv(ΔN89β-Catenin) Epithelium

Chimeric-transgenic animals generated from three of the four ES cell lines were characterized further. All had similar phenotypes. There were no statistically significant differences between the growth rates or adult body weights of chimeric-transgenic and normal chimeric mice (n = 72).

Surveys of X-Gal–stained intestinal wholemounts from 1.5-, 6-, and 10-mo-old chimeric-transgenic mice (n = 1–8 animals/line per time point) revealed that the β-gal–negative 129/Sv(ΔN89β-catenin) epithelium contained branched villi. Typically, there were two branches per villus, each of equivalent height. Branched villi were similar in height to surrounding unbranched villi (Fig. 3, *A* and *B*). When polyclonal villi were encountered with branching, there was always a wholly 129/Sv(ΔN89β-catenin) branch (Fig. 3 *C*).

The frequency of villus branching was quantitated by examining serial sections of X-Gal–stained jejunal wholemounts from 6-mo-old chimeric-transgenic and normal chimeric mice. An average of 3,400 villi were scored per animal using the criteria described in Materials and Methods (n = two or three animals/line). The percentage of branched villi detected in 129/Sv(ΔN89β-catenin) jejunal epithelium ranged from 0.5 to 2%, depending upon the *Fabpl*–ΔN89β-catenin ES cell line used to produce the chimeras (Fig. 4). In contrast, the frequency of villus branching in their B6-ROSA26 jejunal epithelium was <0.01%. This difference was statistically significant ($P < 0.05$). Branched villi were extremely rare (<0.01%) in both the 129/Sv and B6-ROSA26 components of jejunum harvested from aged-matched normal control chimeras (Fig. 4). Villus branching remained confined to the 129/Sv epithelium of 10-mo-old chimeric-transgenic mice (n = 20). The frequency of branching was similar to that observed in 6-mo-old mice.

ΔN89β-Catenin Expression Is Associated with Alterations in Proliferation, Apoptosis, and Migration but Not in Cell Fate Specification or Differentiation

Histochemical stains, plus a panel of antibodies and lectins (refer to Materials and Methods), were used to determine whether the epithelium overlying 129/Sv(ΔN89β-catenin) crypt-villus units exhibited any changes in differentiation. Epithelial cells were compared in adjacent 129/Sv and B6-ROSA26 jejunal crypt-villus units, or within a single polyclonal villus, in both chimeric-transgenic and normal control chimeric mice. Expression of ΔN89β-catenin was not associated with any detectable perturbations in cell fate specification or in the terminal differentiation programs of the enterocytic, enteroendocrine, goblet, or Paneth cell lineages. Cell polarity appeared unaffected in the enterocytic lineage, as judged by the intracellular distribution of actin or by the distribution of apical- and Golgi membrane–associated glycoconjugates (Fig. 5 *A*, for example). The subcellular and crypt-villus distributions of the tight junction protein ZO-1 were similar in the 129/Sv and B6 components of polyclonal villi (Fig. 5 *C*). In addition, there were no discernible changes in the levels or crypt-villus distributions of α_6, β_1, β_4, or β_7 integrin subunits, laminin, fibronectin, or type IV collagen (Fig. 5, *B* and *D;* data not shown).

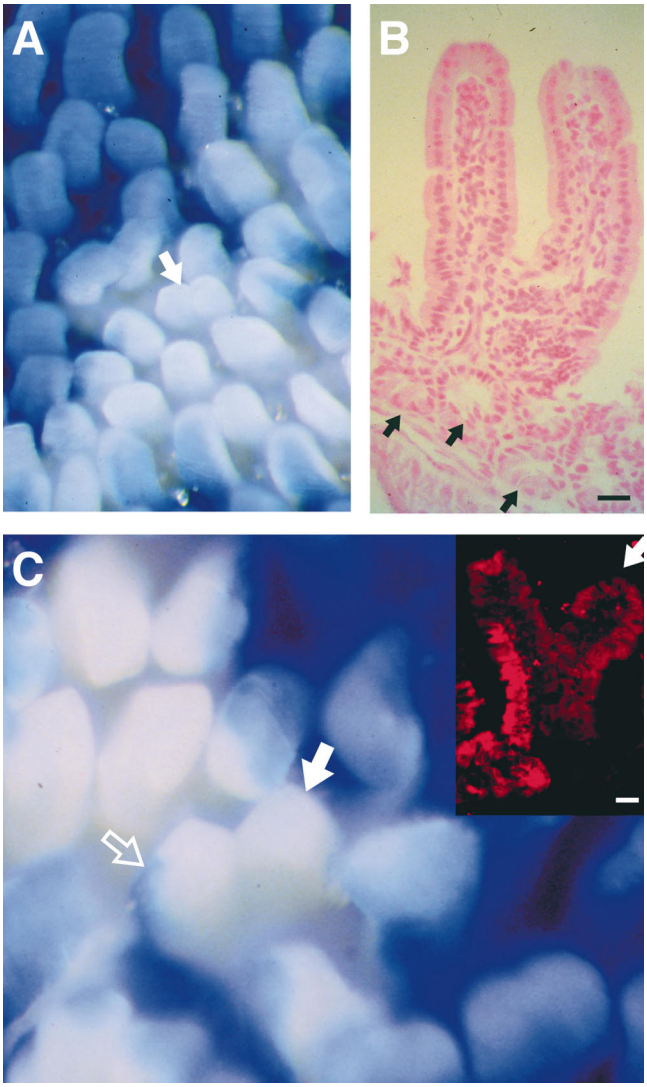

Figure 3. Villus branching in 129/Sv(ΔN89β-catenin) epithelium. (*A*) Wholemount preparation of the jejunum from a 6-mo-old chimeric-transgenic mouse. *Arrow,* branched 129/Sv villus. (*B*) Section from the same wholemount stained with nuclear fast red. Each limb of the branched villus is equivalent in height. There are no obvious morphologic abnormalities in the crypts associated with this villus (*arrows*). (*C*) A branched polyclonal villus. *Open arrow,* a stripe of β-gal–positive (*blue*) B6-ROSA26 epithelium in one of the branches. The other branch is wholly 129/Sv (*closed arrow*; *white*). *Inset*, section of the branched villus incubated with rabbit antibodies to β-gal and Cy3-conjugated donkey anti–rabbit Ig. The stripe of B6-ROSA26 epithelium in one of the branches appears red. *Closed arrow,* the other, β-gal–negative, 129/Sv branch. Bars: (*B* and *C*) 25 μm.

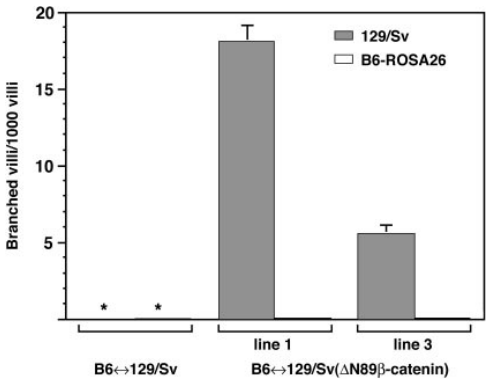

Figure 4. Quantitation of villus branching. Branching was defined and quantitated as described in Materials and Methods. Branched villi were scored in the B6-ROSA26 and 129/Sv jejunal components of 6-mo-old normal chimeras (B6-ROSA26↔129/Sv) and chimeric-transgenic (B6-ROSA26↔129/Sv[NΔ89β-catenin]) mice. Each line of chimeric-transgenic mice was derived from an independent clone of ES cells stably transfected with *Fabpl*–NΔ89β-catenin DNA. Mean values ±1 SD are plotted. *Asterisk*, the frequency of branched villi was <0.01%.

To determine the effects of ΔN89β-catenin on cellular proliferation, M-phase cells were scored in jejunal crypt-villus units of 6-mo-old chimeric-transgenic or normal chimeric mice. The ratio of M-phase cells in adjacent patches of 129/Sv and B6-ROSA26 crypts was calculated for each mouse in each line. Values obtained from all animals in a given line were then averaged (n = 400–600 crypts scored/mouse per line; n = two or three mice/line). Fig. 6 *A* shows there was a statistically significant two- to fourfold increase in the mitotic ratio (index) in chimeric-transgenic mice compared with age-matched normal chimeras ($P < 0.05$). This was due to an increase in the number of M-phase cells per 129/Sv(Δ89β-catenin) crypt section. There were no statistically significant differences in the number of M-phase cells in the B6-ROSA26 crypts of chimeric-transgenic and normal chimeric mice (data not shown). The proliferative abnormality produced by ΔN89β-catenin was confined to the crypt epithelium; no M-phase cells were noted on villi with normal morphology or with a branched phenotype.

A crypt apoptotic index was also defined in these animals. Like the mitotic index, this index was expressed as the ratio of apoptotic cells in adjacent patches of 129/Sv and B6-ROSA26 crypts. An increase in apoptosis, equivalent to the increase in proliferation, was observed in 129/Sv(ΔN89β-catenin) jejunal crypts (Fig. 6 *B*). There were no statistically significant differences in the number of apoptotic cells between the jejunal B6-ROSA26 crypts of chimeric-transgenic and normal control chimeric animals (data not shown).

The effect of ΔN89β-catenin expression on cell migra-

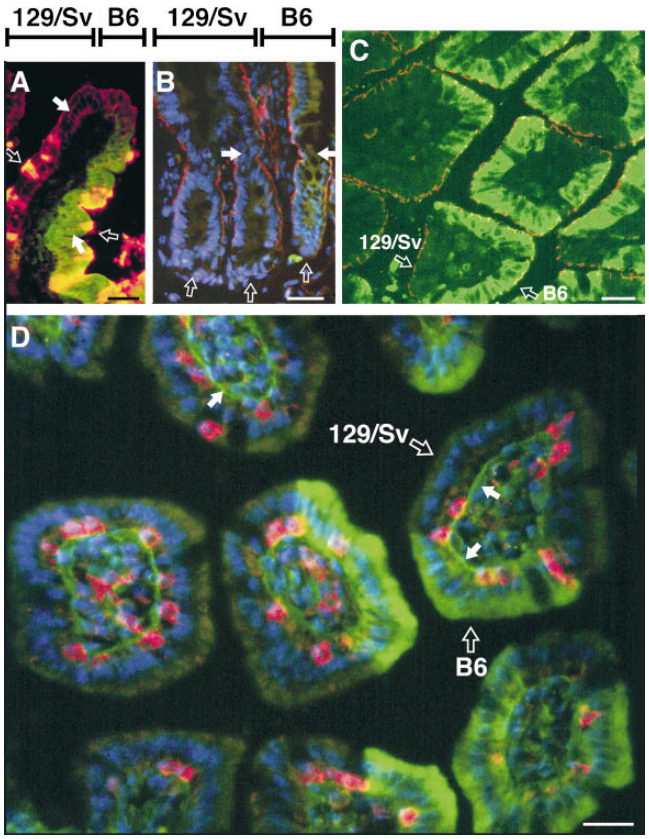

bit anti–β-gal, and FITC-conjugated donkey anti–rabbit Ig. Glycoconjugates containing GalNAcα3GalNAc and GalNAcα3Gal recognized by DBA appear yellow-orange; β-gal appears green. The polarity and differentiation of enterocytes appears to be unaffected, as judged by the distribution of these glycoconjugates in apical membranes and supranuclear Golgi apparatus (*closed arrow*). Similarly, based on their reaction with DBA, the number and differentiation of goblet cells (*open arrows*) is equivalent in the 129/Sv and B6-ROSA26 components of the polyclonal villus. (*B*) The base of a polyclonal villus with its crypt-villus junction indicated by *closed arrows*. Three crypts are seen (*open arrows* at their base): the one on the left is supplying cells to another villus. The section was incubated with rat anti-β_4 integrin subunit, Cy3 donkey anti–rat Ig, rabbit anti–β-gal, FITC donkey anti–rabbit Ig, and bis-benzimide. Nuclei (*blue*); the β_4 integrin subunit (*orange*); β-gal (*green-brown*). The location of β_4 integrin at the base of epithelial cells and its distribution along the crypt-villus unit are unaffected by ΔN89β-catenin. (*C*) Villi sectioned perpendicular to their crypt-villus axis. The tight junction protein ZO-1 (*orange*) was detected with rat anti-ZO-1 and Cy3 donkey anti–rat Ig. β-Gal (*green*) was visualized with the same reagents used in the preceding sections. The levels and location of ZO-1 in the 129/Sv(ΔN89β-catenin) and B6-ROSA26 components of polyclonal villi are similar (e.g., *open arrows*). (*D*) Villi sectioned perpendicular to their crypt-villus axis as in *C*. The section was incubated with rat anti-β_7 integrin, Cy3-donkey anti–rat Ig, rabbit anti-laminin, rabbit anti–β-gal, FITC donkey anti–rabbit Ig, and bis-benzimide. B6-ROSA26 cells exhibit diffuse staining of their cytoplasm due to the presence of β-gal (*green*). β_7 integrin is confined to intraepithelial lymphocytes (*orange*). Comparable numbers of these cells are seen in the B6-ROSA26 and 129/Sv(ΔN89β-catenin) components of polyclonal villi and in wholly 129/Sv(ΔN89β-catenin) villi. Laminin appears as linear green immunoreactivity underlying 129/Sv and B6-ROSA26 epithelium (e.g., *closed arrows*). The intensity of staining is similar under cells of both genotypes. Bars, 25 μm.

Figure 5. Forced expression of ΔN89β-catenin has no discernible effects on epithelial cell differentiation. Frozen sections were prepared from PLP-fixed jejunums of 6-mo-old chimeric-transgenic animals. (*A*) A polyclonal villus stained with biotin-conjugated *Dolichos biflorus* agglutinin (*DBA*), Cy3-conjugated avidin, rab-

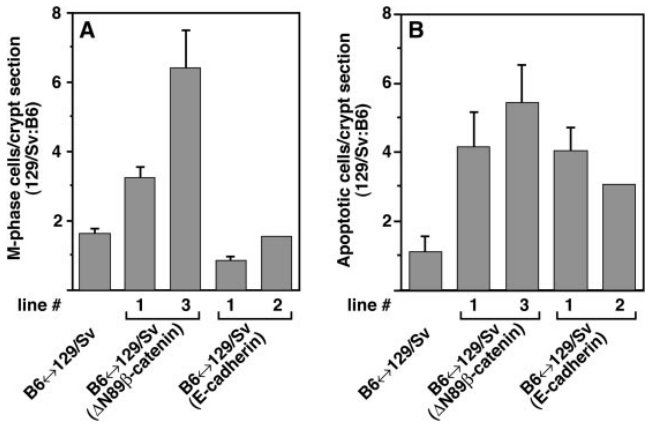

Figure 6. ΔN89β-catenin stimulates proliferation and apoptosis in 129/Sv crypts. (*A*) The number of M-phase cells in juxtaposed B6-ROSA26 and 129/Sv jejunal crypt sections were scored in 6-mo-old normal chimeras, in two lines of chimeric-transgenic mice generated using separate ES cell clones stably transfected with *Fabpl*–ΔN89β-catenin DNA, and in two lines of chimeric-transgenic mice produced from independent ES cells clones stably transfected with *Fabpl*-mouse E-cadherin DNA (Hermiston et al., 1996). Each mouse served as its own control: the average number of M-phase cells in their 129/Sv crypts were divided by the average number of M-phase cells in their B6-ROSA26 crypts. Mean values ±1 SD obtained from animals in each group are plotted except for line 2 of B6↔129/Sv (*E-cadherin*) chimeras where only two animals were examined. Note that the stimulation of crypt proliferation is similar in mice belonging to a given line of B6-ROSA26↔129/Sv(ΔN89β-catenin) chimeras. Differences between lines produced from different *Fabpl*–ΔN89β-catenin ES cell clones were attributed to differences in the levels of expression of this transgene. (*B*) Apoptotic cells were scored in jejunal sections prepared from the same animals used to define the mitotic index in *A*.

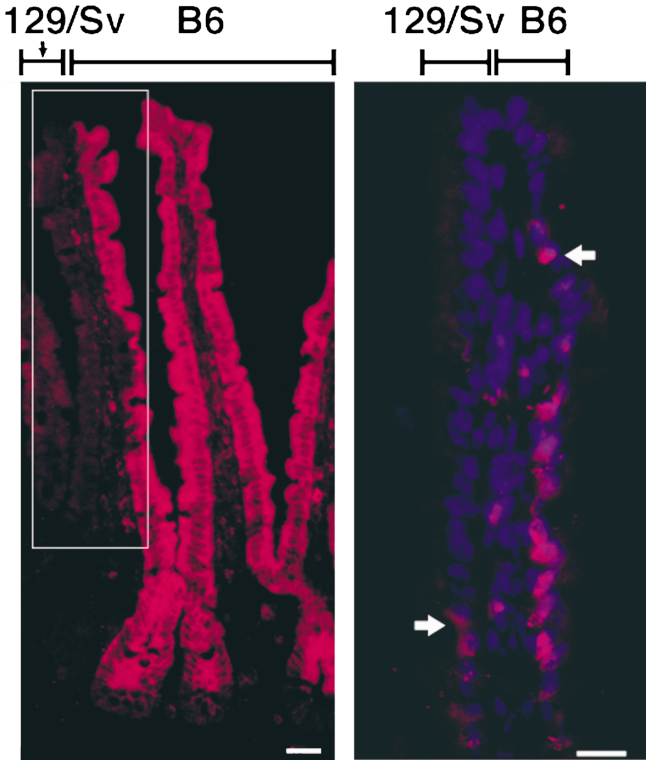

Figure 7. Forced expression of ΔN89β-catenin is associated with a slowing of epithelial migration. A 6-mo-old chimeric-transgenic mouse was pulse labeled with BrdU 60 h before killing. *Left*, a section stained with rabbit anti–β-gal and Cy3 donkey anti–rabbit Ig. The villus encompassed by the box is polyclonal. *Right*, an adjacent section of the polyclonal villus, stained with goat anti-BrdU, Cy3 donkey anti–goat Ig, and bis-benzimide. The leading edge of the column of BrdU–positive 129/Sv(ΔN89β-catenin) epithelial cells (*magenta-colored nuclei*) has only reached the middle portion of the villus (*arrow*), whereas the leading edge of the BrdU–positive B6-ROSA26 column is already near the villus tip. Bars, 25 μm.

tion was also examined. 6-mo-old chimeric-transgenic and normal control chimeric mice were injected with BrdU to label crypt epithelial cells in S phase. Animals were killed 60 h later (n = two mice/line). Serial sections were prepared from their jejunums and then the sections were stained with antibodies to β-gal and BrdU. Analysis of polyclonal villi present in chimeric-transgenic mice revealed a marked difference in migration between 129/Sv(ΔN89β-catenin) and B6-ROSA26 epithelial cells. 60 h after pulse labeling, the leading edge of BrdU-positive B6 cells had moved from the crypt to the upper quarter of the villus, whereas the leading edge of BrdU-positive 129/Sv(ΔN89β-catenin) cells had only reached the middle portion of the villus (Fig. 7). This effect was related to forced expression of ΔN89β-catenin: control studies revealed that there were no detectable differences in migration between 129/Sv and B6-ROSA26 epithelial cells located in the polyclonal villi of normal chimeras (for illustration see Hermiston et al., 1996). Based on previous determinations of the time it takes BrdU-tagged cells to move from the crypt to the villus tip (Hermiston et al., 1996), the observed difference represents a slowing of 129/Sv(ΔN89β-catenin) cell migration by ~12–24 h.

Comparisons of polyclonal jejunal villi present in the wholemount preparations of chimeric-transgenic and normal control chimeric mice (refer to Fig. 1 *A* and Fig. 3, *A* and *C*) established that forced expression of ΔN89β-catenin did not affect the orderliness of migration. The borders between adjacent columns of B6 and 129/Sv(ΔN89β-catenin) epithelium were sharp. There was no sign of infiltration of 129/Sv(ΔN89β-catenin) epithelial cells into adjacent B6-ROSA26 cellular columns, as was seen when the same *Fabpl* transcriptional regulatory elements were used to force expression of wild-type human APC (Wong et al., 1996). Hematoxylin- and eosin-stained sections failed to disclose any piling up of cells at the junctions of 129/Sv(ΔN89β-catenin) crypts and their associated villi. Similarly, there was no aberrant accumulation of cells at the villus tip where cell extrusion normally occurs.

The slowing of migration was not accompanied by any detectable perturbations in contacts between epithelial cells. There was no evidence of disrupted mucosal barrier function: (*a*) surveys of hematoxylin- and eosin-stained jejunal sections from 6-mo-old chimeric-transgenic mice failed to show any signs of inflammatory bowel disease; and (*b*) immunohistochemical analyses indicated that the number and crypt-villus distributions of several components of the diffuse gut–associated lymphoid tissue were unperturbed (e.g., β_7-positive intraepithelial lymphocytes,

$CD4^+$ T cells, and $CD8^+$ T cells; refer to Fig. 5 *D* plus data not shown).

Because aberrant β-catenin signaling has been implicated in the pathogenesis of intestinal neoplasia (refer to *Introduction*), we carefully surveyed X-Gal–stained whole-mounts and serial sections of the small intestine from chimeric-transgenic animals for evidence of dysplasia, adenoma formation, or adenocarcinoma. None of the mice had any evidence of these pathologic changes (n = 72; ages 1.5–10 mo).

Mechanistic Analyses: ΔN89β-Catenin Expression Is Associated with an Augmentation in Cellular Pools of E-Cadherin

Conventional light microscopic and confocal microscopic surveys of jejunal sections, prepared from chimeric-transgenic mice and stained with antibodies against the myc tag or β-catenin, failed to disclose ΔN89β-catenin and endogenous β-catenin in the nuclei of transgenic 129/Sv or normal B6-ROSA26 epithelial cells (refer to Fig. 2 *C* and see Fig. 8 *A*). β-Catenin was present at the adherens junctions and basolateral surfaces of epithelial cells (Fig. 8 *A*).

We examined whether forced expression of ΔN89β-catenin affected the intracellular distribution or levels of its known partners APC, E-cadherin, or α-catenin. To do so, jejunal sections were incubated with antibodies to each protein. Surveys of adjacent 129/Sv(ΔN89β-catenin) and B6-ROSA26 crypt-villus units, as well as polyclonal villi, failed to disclose any appreciable differences in APC or α-catenin localization or levels. α-Catenin remained associated with adherens junctions and the basolateral surfaces of 129/Sv(ΔN89β-catenin) epithelial cells (data not shown), whereas APC was prominent at the periphery of villus epithelial cells where it appeared to form small granular aggregates (Fig. 8 *B*).

In contrast, the steady-state level of E-cadherin was markedly increased in ΔN89β-catenin–producing epithelial cells (Fig. 8, *C* and *D*). The augmented concentration of E-cadherin was not accompanied by detectable changes in its intracellular location (adherens junctions and basolateral surfaces). Analysis of polyclonal jejunal villi from normal chimeras established that the increased level of E-cadherin was not simply due to genotypic differences between 129/Sv and B6-ROSA26 epithelium (Fig. 8, *E* and *F*).

Previous studies, using the same *Fabpl* transcriptional regulatory elements used in this report, had shown that forced expression of wild-type E-cadherin in the jejunal crypt-villus units of chimeric-transgenic mice produced a slowing of epithelial migration equivalent to that observed with ΔN89β-catenin (Hermiston et al., 1996). To determine whether augmented levels of E-cadherin were responsible for the other phenotypic changes observed B6-ROSA26↔129/Sv(ΔN89β-catenin) chimeras, we defined the jejunal crypt mitotic and apoptotic indices in 6-mo-old chimeric-transgenic mice generated using ES cells stably transfected with *Fabpl* mouse E-cadherin DNA (Hermiston et al., 1996). The increase in total M-phase cells/crypt section associated with ΔN89β-catenin expression was not evident in E-cadherin overexpressing crypts (refer to Fig. 6 *A*), indicating that this feature was directly related to ΔN89β-catenin production rather than to a sec-

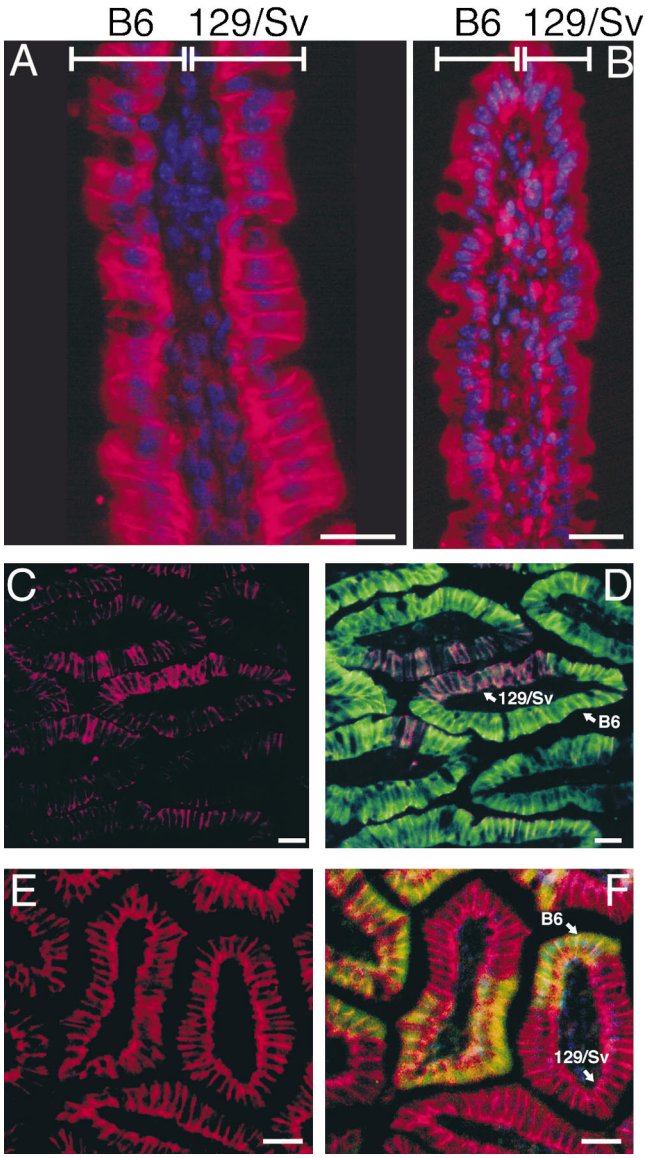

Figure 8. ΔN89β-Catenin expression results in augmented cellular pools of E-cadherin. Frozen sections were prepared from PLP-fixed jejunum recovered from a 6-mo-old B6-ROSA26↔129/Sv(ΔN89β-catenin) chimeric-transgenic animal (*A–D*) and a 6-mo-old normal B6-ROSA26↔129/Sv chimera (*E* and *F*). (*A*) Polyclonal villus incubated with rabbit anti–β-catenin, Cy3 donkey anti–rabbit Ig, and bis-benzimide. Prominent β-catenin staining (*red*) is evident at the adherens junctions and basolateral surfaces of epithelial cells. No immunoreactive protein is detectable in 129/Sv or B6-ROSA26 nuclei. (*B*) Polyclonal villus incubated with rabbit anti-APC, Cy3 donkey anti–rabbit Ig, and bis-benzimide. The levels and intracellular distribution of APC (*red*) are similar in B6-ROSA26 and 129/Sv(ΔN89β-catenin) epithelial cells. (*C* and *D*) Villi from the chimeric-transgenic mouse that have been sectioned perpendicular their crypt-villus axis. (*C*) Section stained with rat anti–E-cadherin and Cy3-donkey anti–rat Ig. (*D*) Dual exposure of the same section after incubation with rabbit anti–β-gal and FITC donkey anti–rabbit Ig. Steady-state levels of E-cadherin are markedly increased in the 129/Sv(ΔN89β-catenin) component of polyclonal villi. (*E* and *F*) Villi from a control normal chimera processed as in (*C* and *D*). E-Cadherin levels are comparable in the B6-ROSA26 and 129/Sv villus epithelium. Bars, 25 μm.

ondary effect of elevated E-cadherin concentrations. We could not make such a statement in the case of the apoptotic response, because similar elevations in crypt apoptosis were associated with forced expression of wild-type E-cadherin and ΔN89β-catenin (Fig. 6 *B*). Forced expression of E-cadherin did not produce villus branching (data not shown).

Discussion

Expression of ΔN89β-catenin, which lacks sites for GSK-3 phosphorylation, can be viewed as simulating at least one effect of active Wnt signaling: generation of augmented cellular pools of stable, hypophosphorylated β-catenin. Comparable NH_2-terminal truncation mutants are known to phenocopy activation of the Wnt signaling pathway in *Xenopus* and *Drosophila*. In these nonmammalian systems, the consequences include axis duplication and changes in cell fate specification (Yost et al., 1996; Pai et al., 1997). Moreover, components in the Wnt signaling pathway play critical roles in specifying endoderm and gut differentiation during early *Caenorhabditis elegans* development (Han, 1997; Rocheleau et al., 1997; Thorpe et al., 1997). ΔN89β-Catenin production in the small intestine of chimeric-transgenic mice was not only designed as an in vivo test of the role of Wnt signaling in establishing and maintaining a self-renewing mammalian epithelium, but also as a test of the effects of β-catenin on a system with complex adhesive requirements (i.e., preservation of cell–cell contacts in a mucosal barrier, orderly yet rapid cell migration, and exfoliation at a defined point in the cellular life cycle).

ΔN89β-Catenin Expression Results in a Proliferative Response Restricted to Crypts

Forced expression of Wnt-1 causes mammary epithelial hyperplasia and tumor formation (Brown et al., 1986; Tsukamoto et al., 1988). In addition, ectopic expression of Wnt-1 enhances proliferation in the developing mammalian central nervous system (Dickinson et al., 1994). The mitogenic response of crypt epithelial cells to ΔN89β-catenin is consistent with the observed mitogenic effects of active Wnt signaling in these other lineages. Surprisingly, this proliferative response was observed in the absence of detectable myc-tagged ΔN89β-catenin (or endogenous β-catenin) within the nucleus of crypt epithelial cells. Forced expression of wild-type β-catenin or ΔN89β-catenin in *Drosophila*, *Xenopus,* two-cell mouse embryos, and cultured mammalian cells has been reported to result in redistribution of β-catenin to the cytoplasm and nucleus (Funayama et al., 1995; Huber et al., 1996; Munemitsu et al., 1996; Yost et al., 1996; Pai et al., 1997). We assume that the amount of immunoreactive β-catenin in the nuclei of crypt epithelial cells was below the limits of detection of our staining techniques.

The proliferative response did not involve villus epithelial cells despite sustained expression of ΔN89β-catenin from the crypt to the villus tip. Studies of nontransgenic mice have shown that these short-lived postmitotic cells retain many critical regulators that allow entry into S phase (e.g., cyclin E and cdk4; Chandrasekaran et al., 1996). Moreover, the villus microenvironment does not impose an absolute prohibition on crossing the G1/S boundary: e.g., villus enterocytes can be induced to undergo a pRB-dependent reentry into the cell cycle by forced expression of SV40 large T antigen (TAg; Chandrasekaran et al., 1996; Coopersmith et al., 1997). The reason why ΔN89β-catenin fails to evoke a proliferative response in villus cells remains unresolved. However, terminal differentiation of these cells may change the availability or function of downstream effectors of the Wnt pathway, such as high motility group box transcription factors.

Primary Versus Secondary Responses: Stimulation of Apoptosis in ΔN89β-Catenin–Producing Crypts and Villus Branching

The intestinal epithelium has a great capacity to initiate compensatory responses that preserve the steady-state cellular census when that census is threatened by changes in proliferative status or cell survival (Hermiston et al., 1995*a*; Coopersmith et al., 1997). As a consequence, it is often difficult to distinguish between primary responses to an applied stimulus and responses that compensate for an effect produced by that stimulus. At this point, we cannot determine whether the apoptosis reflects a direct effect of augmented cytosolic β-catenin pools (and signaling), or a secondary compensatory response to augmented crypt proliferation. Whatever the underlying mechanism, given the lack of discernible effects on villus height, we conclude that the observed changes in cell death are generally able to compensate for the observed changes in cell production.

A quandary exists regarding the interpretation of villus branching. There is little information available about the determinants of villus geometry (Totafurno et al., 1990). For example, are the determinants of morphology primarily epithelial-based or do they also involve mesenchymal signals? The normal variation in villus height observed along the duodenal-ileal axis of the adult mouse intestine can be correlated with the number of crypts that surround the base of each villus (Wright and Irwin, 1982). Totafurno et al. (1987) examined rare branched villi in normal mice and found that the number of crypts that surrounded their base was approximately twice the normal number, suggesting that villus branching may be a compensatory response to increased epithelial cell input. Increased cell production may not have to come from crypts: SV40 TAg expression in villus enterocytes leads to reentry into the cell cycle and branching in a subset of villi (Coopersmith et al., 1997).

We do not view branching as analogous to the axis duplication observed in *Xenopus* when the Wnt pathway is stimulated. It is unclear how a branched shape can be maintained given the perpetual epithelial cell renewal that occurs in crypt-villus units. In fact, the absence of a notable increase in the frequency of villus branching as B6-ROSA26↔129/Sv(ΔN89β-catenin) mice age suggests that branched villi have a limited life span. This is consistent with the view that normal intestine continually produces new crypts and villi as a byproduct of its dynamic cell renewal (Totafurno et al., 1987). Branching in our chimeric-transgenic mice may be a default response, reflect-

ing the inability of some of their villi to adequately compensate for a threatened or real increase in their steady-state epithelial cell census beyond some critical threshold value. Such a threat may arise from the increased cell production observed in their crypts, from the inability of crypt apoptosis to compensate for this proliferative response, and/or from the effects of slowed epithelial cell migration. Branching could also represent a direct response to aberrant signals, originating from a genetically manipulated epithelium and operating through interactions with the underlying mesenchyme. The significance of branching is that it provides a potential inroad to deciphering how villus structure is preserved in the face of perpetual, rapid renewal of its principal cellular component.

ΔN89β-Catenin Produces an Increase in Steady-State Levels of E-Cadherin

Forced expression of ΔN89β-catenin results in a marked increase in E-cadherin levels at the adherens junction and basolateral surfaces of intestinal epithelial cells. Several recent studies suggest that this is due to activation of E-cadherin gene expression. The mouse E-cadherin gene contains a 7-bp binding sequence for Lef-1/Tcf (Huber et al., 1996). Yanagawa and co-workers (1997) used a *Drosophila* wing imaginal disc cell line to show that stimulation of the Wingless pathway induces *Drosophila* E-cadherin gene transcription and accumulation of DE-cadherin at cellular junctions. They also found that forced expression of Dishevelled, an inhibitor of Zeste-white 3 (the *Drosophila* GSK-3 homologue), led to accumulation of Armadillo (the β-catenin homologue) in the cytosol of these cells, a marked increase in *Drosophila* E-cadherin mRNA, and an elevation in junctional DE-cadherin. In addition, they noted that forced expression of an NH_2-terminal truncation mutant of Armadillo produces elevated DE-cadherin mRNA and protein levels.

The ΔN89β-catenin–mediated increase in E-cadherin levels is likely to counteract the signaling activity of ΔN89β-catenin within the intestinal epithelium. Studies in *Xenopus* have shown that the binding of β-catenin to cadherins opposes signaling by sequestering β-catenin (Heasman et al., 1994; Fagotto et al., 1996). The location of myc-tagged ΔN89β-catenin within intestinal epithelial cells provides evidence that a similar process occurs in a mammalian system.

The augmentation in cellular E-cadherin pools is also likely to contribute to the slow migratory phenotype of 129/Sv(ΔN89β-catenin) epithelium. When forced expression of E-cadherin was limited to villus enterocytes in transgenic mice, enterocytic migration from the villus base to villus tip was slowed (Hermiston et al., 1996). In this previous study, there was no augmentation of E-cadherin in the crypt epithelium, no perturbations in crypt proliferation or death, and therefore little likelihood that the observed effect on migration was due to a diminution in net cellular output from the crypt.

APC and the Effects of ΔN89β-Catenin on Intestinal Epithelial Biology

ΔN89β-Catenin production was not associated with any detectable abnormalities in the intracellular distribution or levels of APC within crypt-villus units. This may have contributed to two phenotypic features of our chimeric-transgenic mice: (*a*) slowed migration and (*b*) lack of neoplastic transformation.

Studies in MDCK cells have indicated that β-catenin affects APC's ability to organize microtubules (Näthke et al., 1996; Pollack et al., 1997). ΔN89β-catenin–APC complexes are more stable than wild-type β-catenin–APC complexes, leading to accumulation of ΔN89β-catenin at clusters of APC positioned at the tips of MDCK cell membrane extensions (Näthke et al., 1996; Barth et al., 1997; Pollack et al., 1997). Based on these findings, Pollack and co-workers (1997) proposed that this stabilization of ΔN89β-catenin–APC complexes inhibits (MDCK) migration by somehow perturbing APC function.

Regulation of β-catenin degradation appears to play an important role in colorectal tumorigenesis and in the formation of melanomas (Korinek et al., 1997; Morin et al., 1997; Rubinfeld et al., 1997). Levels of soluble β-catenin are elevated in colon tumor cells (Munemitsu et al., 1995). In addition, mutations in the NH_2 terminus of β-catenin are oncogenic in cultured cells and are associated with intestinal neoplasms (Morin et al., 1997). The stabilized ΔN89β-catenin mutant was produced in intestinal epithelial cells that were able to maintain normal levels of APC. This may account for the failure of these cells to undergo neoplastic transformation during the 10-mo period that animals were studied. In addition, the β-catenin mutations that have been associated with human colorectal cancer involve alterations in NH_2-terminal serine residues. Although it may seem, superficially, that NH_2-terminal truncations would have similar biochemical effects as serine substitution (i.e., protein stabilization), NH_2-terminal phosphorylation may have other roles, including affects on protein–protein interactions that modulate signaling.

Prospectus

The self-renewing intestinal epithelium is able to invoke a variety of compensatory responses when its census is threatened. This capacity to compensate makes sense given the enormous energetic investments required to sustain normal self-renewal. Compensation provides an experimental challenge when trying to decipher the function of molecules such as β-catenin, since dramatic or even noticeable phenotypes may be difficult to elicit. Further analysis of the effects of active β-catenin–mediated signaling on epithelial homeostasis may require forced expression of β-catenin–Lef-1 (or Tcf) fusion proteins or dominant-negative Tcf/Lef-1 mutants (Molenaar et al., 1996). The chimeric-transgenic system described above provides a way of assaying the effects of these mutants in vivo under well-controlled conditions.

We thank D. O'Donnell (Washington University School of Medicine) for expert technical assistance. We are grateful to J. Nelson and P. Polakis for supplying reagents and for their many valuable suggestions during the course of this work.

These studies were supported in part by grants from the National Institutes of Health (DK37960, DK30292, and T32 HlO7275).

Received for publication 4 February 1998 and in revised form 11 March 1998.

References

Aberle, H., S. Butz, J. Stappert, H. Weissig, R. Kemler, and H. Hoschuetzky. 1994. Assembly of the cadherin–catenin complex *in vitro* with recombinant proteins. *J. Cell Sci.* 107:3655–3663.

Aberle, H., A. Bauer, J. Stapper, A. Kispert and R. Kemler. 1997. β-Catenin is a target for the ubiquitin-proteasome pathway. *EMBO (Eur. Mol. Biol. Organ.) J.* 16:3797–3804.

Barth, A.I.M., A.L. Pollack, Y. Altschuler, K.E. Mostov, and W.J. Nelson. 1997. NH_2-terminal deletion of β-catenin results in stable colocalization of mutant β-catenin with APC protein and altered MDCK cell adhesion. *J. Cell Biol.* 136:693–706.

Behrens, J., J.P. von Kries, M. Kühl, L. Bruhn, D. Wedlich, R. Grosschedl, and W. Birchmeier. 1996. Functional interaction of β-catenin with the transcription factor LEF-1. *Nature.* 382:638–642.

Brown, A.M.C., R.S. Wildin, T.J. Prendergast, and H.E. Varmus. 1986. A retrovirus vector expressing the putative mammary oncogene *int*-1 causes partial transformation of a mammary epithelial cell line. *Cell.* 46:1001–1009.

Brunner, E., O. Peter, L. Schweizer, and K. Basler. 1997. *pangolin* encodes a Lef-1 homologue that acts downstream of Armadillo to transduce the Wingless signal in Drosophila. *Nature.* 385:829–833.

Cadigan, K.M., and R. Nusse. 1997. Wnt signaling: A common theme in animal development. *Genes Dev.* 11:3286–3305.

Chandrasekaran, C., C.M. Coopersmith, and J.I. Gordon. 1996. Use of normal and transgenic mice to examine the relationship between terminal differentiation of intestinal epithelial cells and accumulation of their cell cycle regulators. *J. Biol. Chem.* 271:28414–28421.

Cheng, H. 1974*a*. Origin, differentiation and renewal of the four main epithelial cell types in the mouse small intestine. II. Mucous cells. *Am. J. Anat.* 141: 481–502.

Cheng, H. 1974*b*. Origin, differentiation, and renewal of the four main epithelial cell types in the mouse small intestine. IV. Paneth Cells. *Am. J. Anat.* 141:521–536.

Cheng, H., and C.P. Leblond. 1974*a*. Origin, differentiation, and renewal of the four main epithelial cell types in the mouse small intestine. I. Columnar cells. *Am. J. Anat.* 141:461–480.

Cheng, H., and C.P. Leblond. 1974*b*. Origin, differentiation, and renewal of the four main epithelial cell types in the mouse small intestine. III. Entero-endocrine cells. *Am. J. Anat.* 141:503–520.

Cheng, H., and C.P. Leblond. 1974c. Origin, differentiation, and renewal of the four main epithelial cell types in the mouse small intestine. V. Unitarian theory of the origin of the four epithelial cell types. *Am. J. Anat.* 141:537–561.

Cohn, S.A., T.C. Simon, K.A. Roth, E.H. Birkenmeier, and J.I. Gordon. 1992. Use of transgenic mice to map *cis*-acting elements in the intestinal fatty acid binding protein gene (*Fabpi*) that control its cell lineage-specific and regional patterns of expression along the duodenal-colonic and crypt-villus axes of the gut epithelium. *J. Cell Biol.* 119:27–44.

Cook, D., M.J. Fry, K. Hughes, R. Sumathipala, J.R. Woodgett, and T.C. Dale. 1996. Wingless inactivates glycogen synthase kinase-3 via an intracellular signalling pathway which involves a protein kinase C. *EMBO (Eur. Mol. Biol. Organ) J.* 15:4526–4536.

Coopersmith, C.M., C. Chandrasekaran, and J.I. Gordon. 1997. Bitransgenic mice reveal that K-rasVal12 augments a p53-independent apoptosis when small intestinal villus enterocytes reenter the cell cycle. *J. Cell Biol.* 138:167–180.

Cox, R.T., C. Kirkpatrick, and M. Peifer. 1996. Armadillo is required for adherens junction assembly, cell polarity, and morphogenesis during *Drosophila* embryogenesis. *J. Cell Biol.* 134:133–148.

Dickinson, M.E., R. Krumlauf, and A.P. McMahon. 1994. Evidence for a mitogenic effect of Wnt-1 in the developing mammalian central nervous system. *Development (Camb.).* 120:1453–1471.

Fagotto, F., N. Funayama, U. Glück, and B.M. Gumbiner. 1996. Binding to cadherins antagonizes the signaling activity of β-catenin during axis formation in *Xenopus*. *J. Cell Biol.* 132:1105–1114.

Falk, P., K.A. Roth, and J.I. Gordon. 1994. Lectins are sensitive tools for defining differentiation programs of mouse gut epithelial cell lineages. *Am. J. Physiol*. 266:G987–G1003.

Friedrich, G., and P. Soriano. 1991. Promoter traps in embryonic stem cells: a genetic screen to identify and mutate developmental genes in mice. *Genes Dev*. 5:1513–1523.

Funayama, N., F. Fagotto, P. McCrea, and B.M. Gumbiner. 1995. Embryonic axis induction by the armadillo repeat domain of β-catenin: Evidence for intracellular signaling. *J. Cell Biol.* 128:959–968.

Garabedian, E.M., L.J.J. Roberts, M.S. McNevin, and J.I. Gordon. 1997. Examining the role of Paneth cells in the small intestine by lineage ablation in transgenic mice. *J. Biol. Chem.* 272:23729–23740.

Haegel, H., L. Larue, M. Ohsugi, L. Fedorov, K. Herrenknecht, and R. Kemler. 1995. Lack of β-catenin affects mouse development at gastrulation. *Development (Camb.).* 121:3529–3537.

Hall, P.A., P.J. Coates, B. Ansari, and D. Hopwood. 1994. Regulation of cell number in the mammalian gastrointestinal tract: The importance of apoptosis. *J. Cell Sci.* 107:3569–3577.

Han, M. 1997. Gut reaction to Wnt signaling in worms. *Cell.* 90:581–584.

Heasman, J., A. Crawford, K. Goldstone, P. Garner-Hamrick, B. Gumbiner, P. McCrea, C. Kintner, C.Y. Noro, and C. Wylie. 1994. Overexpression of cadherins and underexpression of β-catenin inhibit dorsal mesoderm induction in early *Xenopus* embryos. *Cell.* 79:791–803.

Hermiston, M.L., and J.I. Gordon. 1995*a*. In vivo analysis of cadherin function in the mouse small intestinal epithelium: Essential role in adhesion, maintenance of differentiation, and regulation of programmed cell death. *J. Cell Biol.* 129:489–506.

Hermiston, M.L., and J.I. Gordon. 1995*b*. Inflammatory bowel disease and adenomas in mice expressing a dominant negative N-cadherin. *Science.* 270: 1203–1207.

Hermiston, M.L., M.H. Wong, and J.I. Gordon. 1996. Forced expression of E-cadherin in the mouse small intestinal epithelium slows cell migration and provides evidence for non-autonomous regulation of cell fate in a self-renewing system. *Genes Dev.* 10:985–996.

Hill, H.D., and J.G. Straka. 1988. Protein determination using bicinchoninic acid in the presence of sulfhydryl reagents. *Anal. Biochem.* 170:203–208.

Hinck, L., I.S. Nathke, J. Papkoff, and W.J. Nelson. 1994. Dynamics of cadherin–catenin complex formation: novel protein interactions and pathways of complex assembly. *J. Cell Biol.* 125:1327–1340.

Huber, A.H., W.J. Nelson, and W.I. Weis. 1997. Three-dimensional structure of the armadillo repeat region of β-catenin. *Cell.* 90:871–882.

Huber, O., R. Korn, J. McLaughlin, M. Ohsugi, B.G. Herrmann, and R. Kemler. 1996. Nuclear localization of β-catenin by interaction with transcription factor LEF-1. *Mech. Dev.* 59:3–10.

Ilyas, M., I.P.M. Tomlinson, A. Rowan, M. Pignatelli, and W.F. Bodmer. 1997. β-Catenin mutations in cell lines established from human colorectal cancers. *Proc. Natl. Acad. Sci. USA*. 94:10330-10334.

Jou, T.S., D.B. Stewart, J. Stappert, W.J. Nelson, and J.A. Marrs. 1995. Genetic and biochemical dissection of protein linkages in the cadherin–catenin complex. *Proc. Natl. Acad. Sci. USA*. 92:5067–5071.

Kim, S.H., K.A. Roth, A.R. Moser, and J.I. Gordon. 1993. Transgenic mouse models that explore the multistep hypothesis of intestinal neoplasia. *J. Cell Biol.* 123:877–893.

Kinzler, K.W., and B. Vogelstein. 1996. Lessons from hereditary colorectal cancer. *Cell.* 87:159–170.

Korinek, V., N. Barker, P.J. Morin, D. van Wichen, R. de Weger, K.W. Kinzler, B. Vogelstein, and H. Clevers. 1997. Constitutive transcriptional activation by a β-catenin-Tcf complex in $APC^{-/-}$ colon carcinoma. *Science.* 275:1784–1787.

Laemmli, U.K. 1970. Cleavage of structural proteins during the assembly of the head of bacteriophage T4. *Nature*. 227:680–685.

Loeffler, M., A. Birke, D. Winton, and C. Potten. 1993. Somatic mutation, monoclonality and stochastic models of stem cell organization in the intestinal crypt. *J. Theor. Biol.* 160:471–491.

McCrea, P.D., W.M. Brieher, and B.M. Gumbiner. 1993. Induction of a secondary body axis in *Xenopus* by antibodies to β-catenin. *J. Cell Biol.* 123:477–484.

McLean, I.W., and P.K. Nakane. 1974. Periodate-lysine-paraformaldehyde fixative: A new fixative for immunoelectron microscopy. *J. Histochem. Cytochem*. 22:1077–1083.

Miller, J.R., and R.T. Moon. 1996. Signal transduction through β-catenin and specification of cell fate during embryogenesis. *Genes Dev*. 10:2527–2539.

Molenaar, M., M. van de Wetering, M. Oosterwegel, J. Peterson-Maduro, S. Godsave, V. Korinek, J. Roose, O. Destrée, and H. Clevers. 1996. XTcf-3 transcription factor mediates β-catenin-induced axis formation in *Xenopus* embryos. *Cell.* 86:391–399.

Morin, P.J., A.B. Sparks, V. Korinek, N. Barker, H. Clevers, B. Vogelstein, and K.W. Kinzler. 1997. Activation of β-catenin-Tcf signaling in colon cancer by mutations in β-catenin or APC. *Science.* 275:1787–1790.

Munemitsu, S., I. Albert, B. Souza, B. Rubinfeld, and P. Polakis. 1995. Regulation of intracellular β-catenin levels by the adenomatous polyposis coli (APC) tumor-suppressor protein. *Proc. Natl. Acad. Sci. USA*. 92:3046–3050.

Munemitsu, S., I. Albert, B. Rubinfeld, and P. Polakis. 1996. Deletion of an amino-terminal sequence stabilizes β-catenin *in vivo* and promotes hyperphosphorylation of the adenomatous polyposis coli tumor suppressor protein. *Mol. Cell. Biol.* 16:4088–4094.

Nagafuchi, A., and M. Takeichi. 1988. Cell binding function of E-cadherin is regulated by the cytoplasmic domain. *EMBO (Eur. Mol. Biol. Organ.) J.* 7:3679–3684.

Näthke, I.S., C.L. Adams, P. Polakis, J.H. Sellin, and W.J. Nelson. 1996. The adenomatous polyposis coli tumor suppressor protein localizes to plasma membrane sites involved in active cell migration. *J. Cell Biol.* 134:165–179.

Noordermeer, J., J. Klingensmith, N. Perrimon, and R. Nusse. 1994. Dishevelled and armadillo act in the wingless signalling pathway in *Drosophila*. *Nature.* 367:80–83.

Nusse, R. 1997. A versatile transcriptional effector of *Wingless* signaling. *Cell.* 89:321–323.

Orsulic, S., and M. Peifer. 1996. An in vivo structure-function study of armadillo, the β-catenin homologue, reveals both separate and overlapping regions of the protein required for cell adhesion and for wingless signaling. *J. Cell Biol.* 134:1283–1300.

Overduin, M., T.S. Harvey, S. Bagby, K.I. Tong, P. Yau, M. Takeichi, and M. Ikura. 1995. Solution structure of the epithelial cadherin domain responsible for selective cell adhesion. *Science.* 267:386–389.

Ozawa, M., H. Baribault, and R. Kemler. 1989. The cytoplasmic domain of the cell adhesion molecule uvomorulin associates with three independent proteins structurally related in different species. *EMBO (Eur. Mol. Biol. Organ.) J.* 8:1711–1717.

Ozawa, M., M. Ringwald, and R. Kemler. 1990. Uvomorulin-catenin complex formation is regulated by a specific domain in the cytoplasmic region of the cell adhesion molecule. *Proc. Natl. Acad. Sci. USA*. 87:4246–4250.

Pai, L.-M., S. Orsulic, A. Bejsovec, and M. Peifer. 1997. Negative regulation of Armadillo, a wingless effector in drosophila. *Development (Camb.)*. 124: 2255–2266.

Pollack, A.L., A.I.M. Barth, Y. Altschuler, W.J. Nelson, and K.E. Mostov. 1997. Dynamics of β-catenin interactions with APC protein regulate epithelial tubulogenesis. *J. Cell Biol.* 137:1651–1662.

Potten, C.S., C. Booth, and D.M. Pritchard. 1997. The intestinal epithelial stem cell: the mucosal governor. *Int. J. Exp. Path.* 78:219–243.

Riese, J., X. Yu, A. Munnerlyn, S. Eresh, S.-C. Hsu, R. Grosschedl, and M. Bienz. 1997. LEF-1, a nuclear factor coordinating signaling inputs from *wingless* and *decapentaplegic*. *Cell.* 88:777–787.

Rimm, D.L., E.R. Koslov, P. Kebriaei, C.D. Cinanci, and J.S. Morrow. 1995. α_1(E)-Catenin is an actin-binding and -bundling protein mediating the attachment of F-actin to the membrane adhesion complex. *Proc. Natl. Acad. Sci. USA*. 92:8813–8817.

Rocheleau, C.E., W.D. Downs, R. Lin, C. Wittmann, Y. Bei, Y.-H. Cha, M. Ali, J.R. Priess, and C.C. Mello. 1997. Wnt signaling and an APC-related gene specify endoderm in early *C. elegans* embryos. *Cell.* 90:707–716.

Rubinfeld, B., B. Souza, I. Albert, O. Müller, S.H. Chamberlain, F.R. Masiarz, S. Munemitsu, and P. Polakis. 1993. Association of the *APC* gene product with β-catenin. *Science.* 262:1731–1734.

Rubinfeld, B., I. Albert, E. Porfiri, C. Fiol, S. Munemitsu, and P. Polakis. 1996. Binding of GSK3β to the APC-β-catenin complex and regulation of complex assembly. *Science.* 272:1023–1026.

Rubinfeld, B., P. Robbins, M. El-Gamil, I. Albert, E. Porfiri, and P. Polakis. 1997. Stabilization of β-catenin by genetic defects in melanoma cell lines. *Science.* 275:1790–1792.

Schmidt, G.H., M.M. Wilkinson, and B.A.J. Ponder. 1985. Cell migration pathway in the intestinal epithelium: An *in situ* marker system using mouse aggregation chimeras. *Cell.* 40:425–429.

Shapiro, L., A.M. Fannon, P.D. Kwong, A. Thompson, M.S. Lehmann, G. Grübel, J.-F. Legrand, J. Als-Nielsen, D.R. Colman, and W.A. Hendrickson. 1995. Structural basis of cell-cell adhesion by cadherins. *Nature.* 374:327–386.

Shibata, H., K. Toyama, H. Shioya, M. Ito, M. Hirota, S. Hasegawa, H. Matsumoto, H. Takano, T. Akiyama, K. Toyoshima, R. Kanamaru, Y. Kanegae, I. Saito, Y. Nakamura, K. Shiba, and T. Noda. 1997. Rapid colorectal adenoma formation initiated by conditional targeting of the *Apc* gene. *Science.* 278: 120–123.

Simon, T.C., K.A. Roth, and J.I. Gordon. 1993. Use of transgenic mice to map *cis*-gut elements in the liver fatty acid-binding protein gene (*Fabpl*) that regulate its cell lineage-specific, differentiation-dependent, and spatial patterns of expression in the intestinal epithelium and in the liver acinus. *J. Biol. Chem*. 268:18345–18358.

Su, L.-K., K.W. Kinzler, B. Vogelstein, A.C. Preisinger, A.R. Moser, C. Luongo, K.A. Gould, and W.F. Dove. 1992. Multiple neoplasia caused by a mutation in the *Murine* homolog of the APC gene. *Science.* 256:668–670.

Su, L.-K., B. Vogelstein, and K.W. Kinzler. 1993. Association of the APC tumor suppressor protein with catenins. *Science.* 262:1734–1737.

Sweetser, D.A., E.H. Birkenmeier, P.C. Hoppe, D.W. McKeel, and J.I. Gordon. 1988. Mechanisms underlying generation of gradients in gene expression within the intestine: an analysis using transgenic mice containing fatty acid binding protein-human growth hormone fusion genes. *Genes Dev.* 2:1318–1332.

Thorpe, C.J., A. Schlesinger, J.C. Carter, and B. Bowerman. 1997. Wnt signaling polarizes an early *C. elegans* blastomore to distinguish endoderm from mesoderm. *Cell.* 90:695–705.

Totafurno, J., M. Bjerknes, and H. Cheng. 1987. The crypt cycle: crypt and villus production in the adult intestinal epithelium. *Biophys. J.* 52:279–294.

Totafurno, J., M. Bjerknes, M.J. Allen, and H. Cheng. 1990. Theoretical analysis of the flow of cells over villi of the small intestine. *J. Math. Biol.* 28:567–584.

Trahair, J., M. Neutra, and J.I. Gordon. 1989. Use of transgenic mice to study the routing of secretory proteins in intestinal epithelial cells: Analysis of human growth hormone compartmentation as a function of cell type and differentiation. *J. Cell Biol.* 19:3231–3242.

Tsukamoto A.S., R. Grosschedl, R.C. Guzman, T. Parslow, and H.E. Varmus. 1988. Expression of the *int*-1 gene in transgenic mice is associated with mammary gland hyperplasia and adenocarcinomas in male and female mice. *Cell.* 55:619–625.

van de Wetering, M., R. Cavallo, D. Dooijes, M. van Beest, J. van Es, J. Loureiro, A. Ypma, D. Hursch, T. Jones, A. Bejsovec, M. Peifer, M. Mortin, and H. Clevers. 1997. Armadillo coactivates transcription driven by the product of the *Drosophila* segment polarity gene *dTCF*. *Cell.* 88:789–799.

Wong, M.H., M.L. Hermiston, A.J. Syder, and J.I. Gordon. 1996. Forced expression of the tumor suppressor adenomatosis polyposis coli protein induces disordered cell migration in the intestinal epithelium. *Proc. Natl. Acad. Sci. USA*. 93:9588–9593.

Wright, N.A. and M. Irwin. 1982. The kinetics of villus cell populations in the mouse small intestine: Normal villi—the steady state requirement. *Cell Tissue Kinet.* 15:595–609.

Yanagawa, S.-I., J.-S. Lee, T. Haruna, H. Oda, T. Uemura, M. Takeichi, and A. Ishimoto. 1997. Accumulation of armadillo induced by wingless, dishevelled, and dominant-negative zeste-white 3 leads to elevated DE-cadherin in *Drosophila* clone 8 wing disc cells. *J. Biol. Chem.* 272:25243–25251.

Yost, C., M. Torres, J.R. Miller, E. Huang, D. Kimelman, and R.T. Moon. 1996. The axis-inducing activity, stability, and subcellular distribution of β-catenin is regulated in *Xenopus* embryos by glycogen synthase kinase 3. *Genes Dev.* 10:1443–1454.